Bulg. J. Phys. **37** (2010) 215–222

Monte Carlo Based Calculation of Electron Transport Properties in Bulk InAs, AlAs and InAlAs

H. Arabshahi[1], **S. Golafrooz**[2]

[1]Department of Physics, Ferdowsi University of Mashhad, P.O. Box 91775-1436, Mashhad, Iran
[2]Salman Institute of Higher Education, P.O. Box 91376-66111, Mashhad, Iran

Received *25 November 2010*

Abstract. We present Monte Carlo based calculations of electron transport in InAs, AlAs and InAlAs based devices. The calculations are performed using a three valleys ensemble Monte Carlo model that includes numerical formulations of the phonon scattering rates and ionized impurity scattering rates. Calculations are made for the zincblende phase of these materials. For all materials, we find that electron velocity overshoot only occurs when the electric field is increased to a value above a certain critical field. This critical field is strongly dependent on the material parameters. Results from the various materials are finally compared.

PACS number: 72.20.-i, 02.70.Uu

1 Introduction

InAs, AlAs and InAlAs semiconductors are becoming of increasing importance in many emerging optoelectronic and electronic device applications. Among these applications are ultraviolet photodetectors, blue and UV light emitters, and high frequency, high power electronic devices [1–3]. Different InAs/AlAs electronic and optoelectronic devices with quantum effects are currently commercially available. An increasing tendency in such devices is the implementation of complicated multi-layered nano-systems, containing two or more components interacting with each other. Such systems are, for example, the superlattices (SLs) with embedded quantum wells (QWs) [4, 5]. They represent a SL, in which one or more of the QWs are wider or narrower than the others. Improved electron transport properties are one of the main targets in the ongoing study of binary and ternary AlAs and InAlAs materials. The Monte Carlo technique has proved valuable for studying non-equilibrium carrier transport in an arrangement of semiconductor materials and devices [6, 7]. However, carrier transport

modeling of AlAs and InAlAs materials has only recently begun to receive sustained attention, now that the growth of compounds and alloys is able to produce valuable materials for the electronics industry [8, 9]. In this communication, we present Monte Carlo calculations of steady-state electron transport conditions in InAs, AlAs and InAlAs. We demonstrate the effect of injection energy and electric field on the electron transport properties. This paper is organized as follows. Details of the employed simulation model are presented in Section 2 and the results of steady-state electron transport properties carried out on InAs, AlAs and InAlAs structures are interpreted in Section 3.

2 Model Details

Within the framework of the materials theory based modeling methodology [10] the first step in studying the transport parameters of semiconductor materials is the calculation of the electronic structure. The band structures of a number of wide band gap material systems, used within the Monte Carlo simulation are calculated using the empirical pseudopotential method. Though *ab initio* methods have been applied to the study of the band structures of the wide gap semiconductors [11], the empirical pseudopotential method is employed herein since it offers a computationally efficient and reasonably accurate accounting of the band structure. The band structures of several materials are computed for a suitable number of k-points within the irreducible wedge taking into account the symmetry of the different crystalline structures. Values of the energy and group velocity are stored along with their wave functions for a fine grid of k-points lying within the irreducible wedge. The information for all the other points in the first Brillouin zone used in the Monte Carlo simulation is recovered using symmetry transformations. The electron–phonon and impurity scattering form the other principal inputs into the Monte Carlo model. Because most of the semiconductor materials can be grown in different phases, and therefore present different symmetry properties, the scattering rate models need to be carefully chosen. An energy dependent formulation for the scattering rate may not always be the best choice. This is particularly true for the hole transport, where the warping of the valence bands may lead to significant anisotropy making the energy dependent model unsuitable for describing the hole–phonon interaction. The Monte Carlo model employed to study electron transport in the compounds includes polar optical, acoustic phonon, ionized impurity and piezoelectric scattering for energies below the secondary valleys. The acoustic phonon scattering is formulated inelastically. Above the secondary valley, only polar optical and deformation potential scattering are included. This choice is made to avoid using intervalley scattering explicitly since the intervalley deformation potentials are unknown. By substituting a general deformation potential scattering mechanism in place of the many intervalley mechanisms, the parametrization can be greatly reduced. Therefore, only one isotropic deformation potential scattering

mechanism based on the realistic density of states is employed at electron energies above the secondary valley of the first conduction band. The coupling constant for this deformation potential scattering is determined by matching the low energy and high energy rates at a suitable energy. In the hole transport study the situation is different. Although the same mechanisms are used, the dependence of the rate on the k-vector has to be considered owing to the high degree of anisotropy within the valence bands. For cubic materials such as InAs, AlAs and InAlAs, the k-dependence can be introduced by computing the scattering rates in three principal directions and interpolating the values of the rates for all other k-points. In this case the rates for the different mechanisms are computed on a grid of k-points in the irreducible wedge and the values for all other points are determined by a suitable interpolation. The values of the parameters used for different materials have been reported elsewhere [12, 13].

In our Monte Carlo simulation, the Γ valley, the four equivalent L valleys, and the three equivalent X valleys were represented by spherical, non-parabolic, analytical effective mass expressions of the following form [12–14]:

$$E(\mathbf{k})[1 + \alpha_i E(\mathbf{k})] = \frac{\hbar^2 k^2}{2m^*}\,, \tag{1}$$

where m^* is the effective mass at the band edge and α_i is the nonparabolicity coefficient of the *i*-th valley given by Kane model [13] as

$$\alpha_i = \frac{1}{E_g}\left[1 - \frac{2m^*}{m_0}\right]\left[1 - \frac{E_g\Delta}{3(E_g + \Delta)(E_g + 2\Delta/3)}\right], \tag{2}$$

where E_g is the band-gap energy and Δ is the spin-orbit splitting.

3 Results

Figure 1 shows the calculated velocity-field characteristics of zincblende InAs, InAlAs and AlAs semiconductors at 300 K, with a background doping concentration of $10^{17}\mathrm{cm}^{-3}$, and with the electric field applied along one of the cubic axes. The simulations suggest that the peak drift velocity for zincblende InAs is 2.25×10^5 ms^{-1}, while those for InAlAs and AlAs are about $\sim 2.3 \times 10^5$ ms^{-1}, 1×10^5 ms^{-1} and 0.25×10^5 ms^{-1}, respectively. At higher electric fields, intervalley optical phonon emission dominates, causing the drift velocity to saturate at around 0.75×10^5 ms^{-1} for InAS and InAlAs materials.

The calculated drift velocities apparent from Figure 1 are fractionally lower than those that have been calculated by Adachi *et al.* [4–6], who assumed an effective mass in the upper valleys equal to the free electron mass. The threshold field for the onset of significant scattering into satellite conduction band valleys is a function of the intervalley separation and the density of electronic states in the satellite valleys.

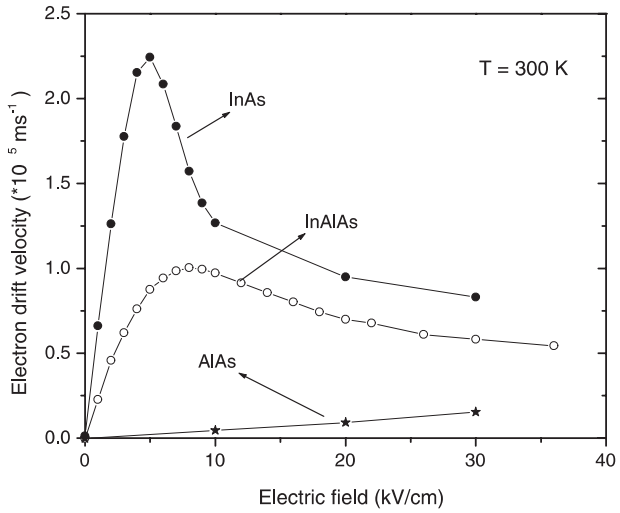

Figure 1. Calculated steady-state electron drift velocity in bulk zincblende InAs, InAlAs and AlAs using nonparabolic band models at room temperature.

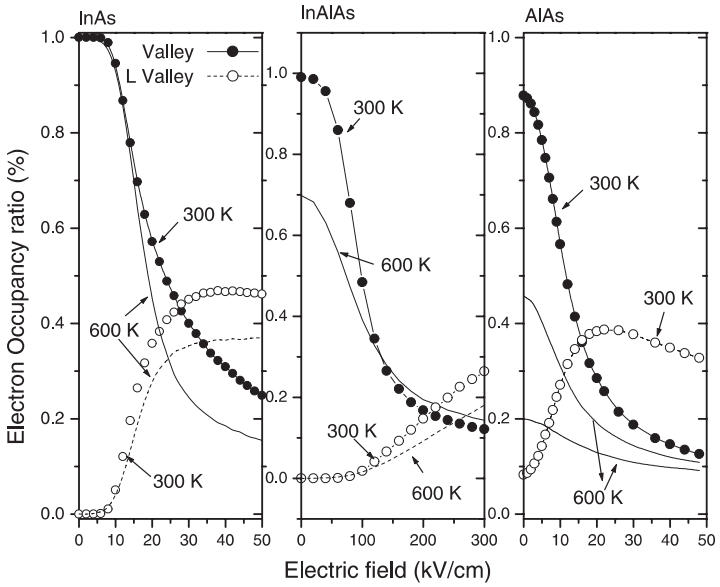

Figure 2. Fractional occupation of the central Γ and satellite valleys of zincblende InAs, InAlAs and AlAs as a function of applied electric field and temperature using the non-parabolic band model.

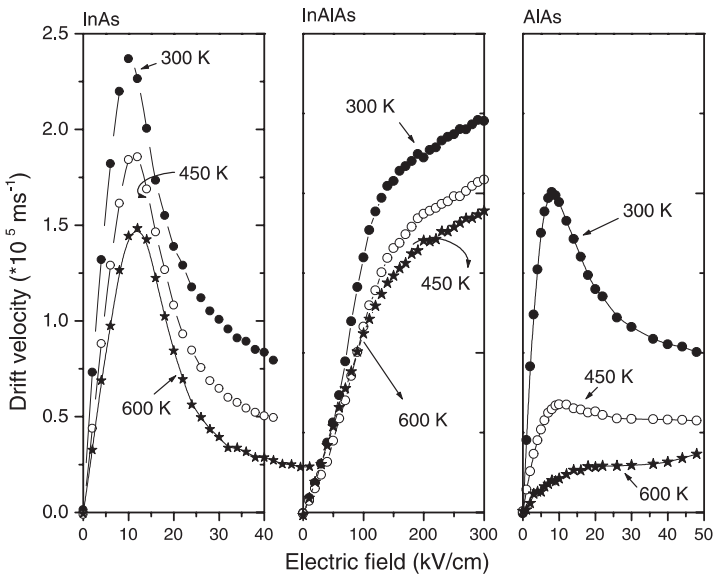

Figure 3. Calculated electron steady-state drift velocity in bulk InAs, InAlAs and AlAs as a function of applied electric field at various lattice temperatures and assuming a donor concentration of 10^{17} cm^{-3}. The peak drift velocity decreases with increasing lattice temperature from 300 to 600 K in all structures.

The valley occupancies for the Γ, X and L valleys are illustrated in Figure 2 and show that the inclusion of the satellite valleys in the simulation is important. Significant intervalley scattering into the satellite valleys occurs for fields above the threshold field for each material. This is important because electrons which are near a valley minimum have small kinetic energies and are therefore strongly scattered. It is apparent that intervalley transfer is substantially larger in InAs over the range of applied electric fields shown, due to the combined effect of a lower Γ effective mass, lower satellite valley separation energy, and slightly lower phonon scattering rate within the Γ valley.

Figure 3 shows the calculated electron drift velocity as a function of electric field strength for temperatures of 300, 450 and 600 K. The decrease in drift mobility with temperature at low fields is due to increased intravalley polar optical phonon scattering whereas the decrease in velocity at higher fields is due to increased intra and intervalley scattering. It can be seen from the figure that the peak velocity also decreases and moves to higher electric field as the temperature is increased. This is due to the general increase of the total scattering rate with temperature, which suppresses the electron energy and reduces the population of the satellite valleys. This latter effect is apparent from the fact that the electron population in the Γ-valley increases with temperature.

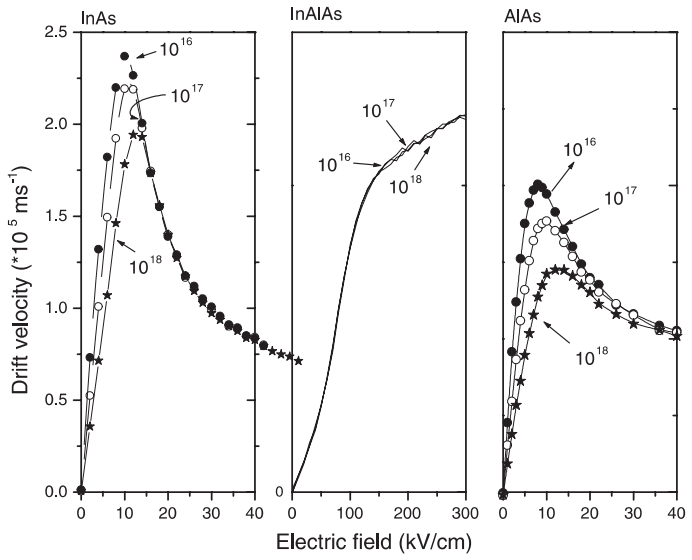

Figure 4. Electric field dependence of the drift velocity in InAs, InAlAs and AlAs at 300 K for various donor concentrations.

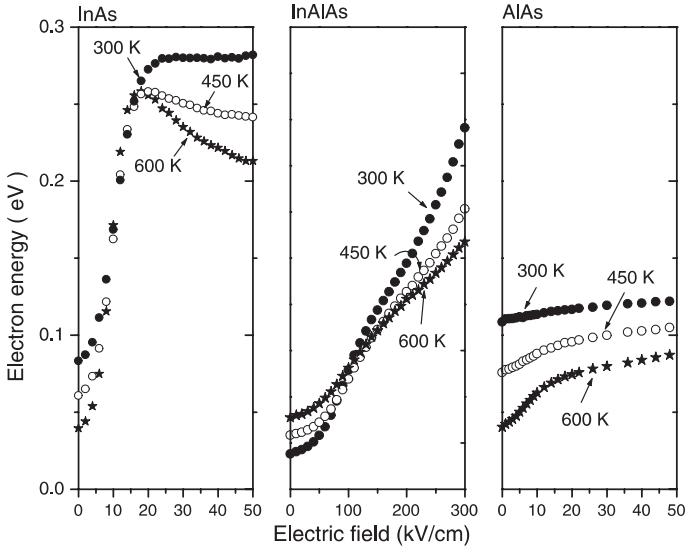

Figure 5. Average electron kinetic energy as function of applied electric field in bulk InAs, InAlAs and AlAs at various temperatures using the nonparabolic band model.

Figure 4 shows how the velocity-field characteristic of InAs, InAlAs and AlAs changes with impurity concentration at 300 K. It is clear that with increasing

donor concentration, there are small changes in the average peak drift velocity and the threshold field. The results show the trend expected from increased ionized impurity scattering is in good general agreement with recent calculations by other workers [14].

The average electron kinetic energy as a function of electric field is shown in Figure 5. The curves have the S-shape typical of III-V compounds, which is a consequence of intervalley transfer. At high fields the average electron energy is decreased due to a higher electron scattering rate. This difference can be understood by considering the Γ-valley occupancy as function of field.

4 Conclusions

The electron transport up to 600 K in bulk InAs, InAlAs and AlAs has been simulated using an ensemble Monte Carlo simulation. Using valley models to describe the electronic bandstructure, calculated velocity-field characteristics are in fair agreement with other calculations. Saturation drift velocities $\sim 0.75 \times 10^5$ ms^{-1} for InAs and InAlAs match recent measurements on low-doped bulk samples. The velocity-field characteristics of the materials show similar trends, reflecting the fact that all the semiconductors have satellite valley effective densities of states several times greater than the central Γ valley. However, the peak velocity in InAlAs occurs at a field $\sim$ 800 kVm^{-1}, 1.3 times larger than for InAs. This is a consequence of the large Γ valley effective mass in InAs structure. This reduced valley effective mass in InAs permits substantial population of the upper valleys and velocity saturation at far lower electron temperatures than in InP.

References

[1] U.V. Bhapkar, M.S. Shur (1997) *J. Appl. Phys.* **82** 1649.

[2] J.D. Albrecht, R.P. Wang, P.P. Ruden, K.F. Brennan (1998) *J. Appl. Phys.* **83** 2185.

[3] E.O. Kane (1957) *J. Phys. Chem. Solids* **1** 249.

[4] S. Adachi (1994) "*GaAs and Related Materials, Bulk Semiconducting and Superlattice Properties*", World Scientific, Singapore.

[5] S. Adachi (1992) "*Physical Properties of III-V Semiconductor Compounds, InP, InAs, GaAs, GaP,AlAs and AlGaAs*", Wiley, New York.

[6] S. Adachi (1993) "*Properties of AlGaAs*", INSPEC, Stevenage, Herts., UK.

[7] K. Brennan, K. Hess, J.Y. Tang, G.J. Iafrate (1983) *IEEE Trans. Electron Devices* **30** 1750.

[8] N. Newman, T. Kendelewicz, L. Bowman, W.E. Spicer (1985) *Appl. Phys. Lett.* **46** 1176.

[9] N. Newman, V. Schilfgaarde, T. Kendelewicz, W.E. Spicer (1986) *Mater. Res. Soc. Symp. Proc.* **54** 443.

[10] D.C. Cameron, L.D. Irving, C.R. Whitehouse (1983) *Thin Solid Films* **103** 61.

[11] D.C. Cameron, L.D. Irving, C.R. Whitehouse (1982) *Electron. Lett.* **18** 534.
[12] C. Moglestue (1993) "*Monte Carlo Simulation of Semiconductor Devices*", Chapman and Hall.
[13] C. Jacoboni, P. Lugli (1989) "*The Monte Carlo Method for Semiconductor and Device Simulation*", Springer-Verlag.
[14] H. Arabshahi, M.R. Benam, B. Salahi (2007) *Mod. Phys. Lett. B* **21** 1715.
[15] H. Arabshahi (2007) *Mod. Phys. Lett. B* **21** 199.
[16] B.E. Foutz, L.F. Eastman, U.V. Bhapkar, M. Shur (1997) *Appl. Phys. Lett.* **70** 2849.